

Direct observation of the energy gap generating the 1/3 magnetization plateau in the spin-1/2 trimer chain compound $\text{Cu}_3(\text{P}_2\text{O}_6\text{OD})_2$ by inelastic neutron scattering measurements

Masashi Hase,^{1,*} Masaaki Matsuda,² Kazuhisa Kakurai,² Kiyoshi Ozawa,¹ Hideaki Kitazawa,¹ Naohito Tsujii,¹ Andreas Dönni,¹ Masanori Kohno,¹ and Xiao Hu¹

¹National Institute for Materials Science (NIMS), 1-2-1 Sengen, Tsukuba, Ibaraki 305-0047, Japan

²Japan Atomic Energy Agency (JAEA), 2-4 Shirakata Shirane, Tokai, Naka, Ibaraki 319-1195, Japan

(Received 3 June 2007; published 29 August 2007)

We studied magnetism of $\text{Cu}_3(\text{P}_2\text{O}_6\text{OD})_2$ using inelastic neutron scattering measurements on a powder sample. This cuprate has spin-1/2 trimer chains with J_1 - J_2 - J_2 interactions, where J_1 and J_2 denote two antiferromagnetic (AF) exchange interaction parameters, showing a 1/3 magnetization plateau. We observed an energy gap of 9.8 meV (114 K), which generated the magnetization plateau. The gap corresponds to singlet-triplet-like excitation of an AF dimer formed by the dominant J_1 interaction. We determined the AF exchange interaction parameters $J_1=111$ K and $J_2=30$ K, which can reproduce the gap value as well as the magnetization.

DOI: 10.1103/PhysRevB.76.064431

PACS number(s): 75.10.Jm, 75.10.Pq, 75.25.+z, 75.50.Ee

I. INTRODUCTION

The magnetization plateau is a notable phenomenon in quantum spin systems. It has been studied extensively during the past decade.¹⁻⁴ The origin of the magnetization plateau is an energy gap in the magnetic excitation spectrum. For that reason, in order to understand the physics of the magnetization plateau, it is necessary to investigate the gap using other methods. A zero-magnetization plateau appears in spin systems possessing a spin-singlet ground state and a gap between the ground and excited states. Examples are Haldane substances,^{5,6} the spin-Peierls cuprate CuGeO_3 ,⁷ and the orthogonal-dimer compound $\text{SrCu}_2(\text{BO}_3)_2$.⁸ Existence of the gap can be proven explicitly by the exponential decay of magnetic susceptibility on cooling without theoretical support.⁸⁻¹⁰ On the contrary, we cannot confirm the existence of a gap, which generates a finite-magnetization plateau, from the temperature dependence of any physical quantity without the aid of theoretical calculations.¹¹⁻¹³

The value of a gap can be evaluated directly using inelastic neutron scattering (INS), electron spin resonance (ESR), and Raman scattering measurements. When a gap value is large, these measurements are valid, while a gap value may not be obtained using magnetization measurements. For example, when a g factor is 2.1, 100 T corresponds to 12.2 meV, 2940 GHz, and 98.4 cm^{-1} , which are not so difficult to attain in the above-mentioned experiments. Among the measurements, it is generally recognized that the INS measurement on single crystals is a powerful tool to study excitations because we can obtain information on scattering vector Q and energy transfer ω dependences. In some cases, the INS measurement on powder samples is also important. For example, we can observe a singlet-triplet gap excitation even in powder samples. In addition, only the INS measurement can directly determine magnetic bonds possessing strong exchange interactions because we can evaluate bond lengths from Q dependence of a scattering intensity.

The INS and ESR measurements have already been used for spin systems showing a finite magnetization plateau. In single crystals of NH_4CuCl_3 having three different spin-1/2

antiferromagnetic (AF) dimers, two gap excitations corresponding to 1/4 and 3/4 magnetization plateaus were observed at 1.6 and 3.0 meV in INS (Ref. 14) and ESR (Ref. 15) measurements. In a single crystal of $\text{Cu}_3(\text{OH})_2(\text{CO}_3)_2$ having a spin-1/2 diamond chain, a gap excitation corresponding to a 1/3 magnetization plateau was observed at 4.4 meV (1057 GHz) in ESR measurements.¹⁶ In principle, a transition between two states with different values of total spin is forbidden in ESR. Observation of the gap excitations, however, is possible because of the antisymmetric Dzyaloshinskii-Moriya interaction. We can say that the direct observations of the gap causing the finite-magnetization plateau are few. Accordingly, experimental investigations are insufficient for understanding the finite-magnetization plateau. It is important to perform further experiments.

Recently, some of the authors of this report found a 1/3 magnetization plateau in $\text{Cu}_3(\text{P}_2\text{O}_6\text{OH})_2$.¹⁷ The space group of $\text{Cu}_3(\text{P}_2\text{O}_6\text{OH})_2$ is $P\bar{1}$ (No. 2); its lattice constants are $a=4.781\,91(6) \text{ \AA}$, $b=7.036\,99(8) \text{ \AA}$, $c=8.357\,40(8) \text{ \AA}$, $\alpha=66.6790(6)^\circ$, $\beta=76.9930(7)^\circ$, $\gamma=72.0642(6)^\circ$, and $Z=1$ (1 formula per unit cell).¹⁸ As shown in Fig. 1, two kinds of Cu^{2+} -ion sites (Cu1 and Cu2) exist and form a spin-1/2 trimer chain nearly parallel to the c direction with J_1 - J_2 - J_2 interactions, where J_1 and J_2 indicate two kinds of AF exchange interaction parameters. Values of J_1 and J_2 were evaluated as 95 and 28 K, respectively, from magnetizations.¹⁷ The J_1 interaction is dominant. Therefore, two spins on Cu2 sites connected by the J_1 interaction form a partial state that resembles a spin-singlet pair (singletlike pair indicated by the ellipse in Fig. 1). It is expected that the main origin of the gap, which causes the 1/3 magnetization plateau, is the singlet-triplet excitation of the AF dimer formed by the dominant J_1 interaction. The value of the gap was calculated as 92 K (8.1 meV). An effective interaction exists between two spins on Cu1 sites through the AF dimer of the Cu2 spins formed by the J_1 interaction. The system consisting of the Cu1 spins behaves as an effective AF uniform chain. The value of the effective interaction was estimated roughly as $J_{\text{eff}} \sim J_2^2/J_1 = 8.0$ K. The moment of the Cu2 spins is very small in the plateau region and in smaller

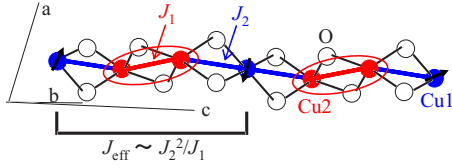


FIG. 1. (Color online) Spin state of $\text{Cu}_3(\text{P}_2\text{O}_6\text{OH})_2$ in a zero magnetic field derived from the results of magnetization. Blue, red, and white circles respectively indicate Cu1 sites, Cu2 sites, and O sites connecting to Cu. Black bars represent Cu-O bonds. Red (blue) bars represent the first shortest (second shortest) Cu-Cu bonds in which the J_1 (J_2) exchange interactions exist. The interaction parameters are defined in the Hamiltonian $\mathcal{H} = \sum_i J_1 S_i S_{i+1} + J_2 S_{i+1} S_{i+2} + J_2 S_{i+2} S_{i+3}$. The J_1 and J_2 interactions form the spin-1/2 trimer (J_1 - J_2 - J_2) chain. The red ellipse denotes a singletlike pair. Spins (black arrows) on the Cu1 sites are coupled to one another by J_{eff} interaction. In the previous study (Ref. 17), the values of J_1 , J_2 , and J_{eff} were evaluated respectively as 95, 28, and 8.0 K. In the present study, we reevaluate the values of J_1 , J_2 , and J_{eff} , respectively, as 111, 30, and 8.1 K.

magnetic fields because of the large gap, while the moment of the Cu1 spins is almost saturated in the plateau region because of the small value of J_{eff} . Accordingly, the 1/3 magnetization plateau can appear.

We have chosen INS measurements to study the gap in a deuterated $\text{Cu}_3(\text{P}_2\text{O}_6\text{OD})_2$ powder sample. The main origin of the gap is expected to be the AF dimer. Therefore, the gap excitation is probably visible even in powder samples, as in INS measurements of a $\text{CaCuGe}_2\text{O}_6$ powder sample.¹⁹ We can evaluate the distance between two spins responsible for the gap from scattering vector Q dependence of scattering intensities if dispersion of the excitation is small. Such an evaluation is impossible using other methods. Consequently, we can verify whether the spin system proposed for $\text{Cu}_3(\text{P}_2\text{O}_6\text{OH})_2$ is correct or not.

II. METHODS OF EXPERIMENTS AND CALCULATION

We synthesized crystalline powder of $\text{Cu}_3(\text{P}_2\text{O}_6\text{OD})_2$ from a mixture of CuO and $\text{D}_3\text{PO}_4\text{-D}_2\text{O}$.¹⁸ The mixture ratios of the two substances are, respectively, 0.5 g: 20 mL for CuO and $\text{D}_3\text{PO}_4\text{-D}_2\text{O}$. The mixture was stirred continuously and heated until CuO was dissolved completely. Then the mixture was kept in a furnace in air at 463 K for 48 h. The $\text{Cu}_3(\text{P}_2\text{O}_6\text{OD})_2$ appeared as a light blue powder. We used x-ray diffraction measurements to confirm the formation of $\text{Cu}_3(\text{P}_2\text{O}_6\text{OD})_2$ and the absence of other materials. We measured magnetizations using a superconducting quantum interference device magnetometer (MPMS-5S, Quantum Design). High-field magnetizations up to 30 T were measured using an extraction-type magnetometer in a hybrid magnet at the High Magnetic Field Center, NIMS. The magnetization of $\text{Cu}_3(\text{P}_2\text{O}_6\text{OD})_2$ is identical to that of $\text{Cu}_3(\text{P}_2\text{O}_6\text{OH})_2$ within experimental accuracy.

Inelastic neutron scattering measurements were carried out on the thermal neutron three-axis spectrometer TAS-2 installed at JRR-3 at the Japan Atomic Energy Agency. The

final neutron energy was fixed at 13.7 meV. Higher-order beam contamination was effectively eliminated using a pyrolytic graphite filter after the sample. The horizontal collimator sequence was guide-80'-sample-80'-open. This setup yields an energy resolution of 1.76 meV (full width at half maximum) at an energy transfer $\omega=0$ meV, as determined from measuring the incoherent scattering from the sample. The powder sample of about 9 g was mounted in a ⁴He closed cycle refrigerator.

We calculated the susceptibility and magnetization of trimer chains by quantum Monte Carlo (QMC) techniques using the loop algorithm²⁰ and using the directed-loop algorithm in the path-integral formulation,²¹ respectively. The numbers of Cu sites in the QMC simulations are respectively 200 and 120 for the temperature dependence of the susceptibility and magnetic-field dependence of magnetization. We performed more than 10^6 updates. Finite-size effects and statistical errors are negligible for the scale of figures represented in this paper.

III. RESULTS AND DISCUSSION

The open circles in Fig. 2(a) show constant- Q scan spectra taken at a temperature of $T=5.1$ K and several scattering vectors (Q 's). In each spectrum, a well-defined symmetric inelastic peak is observed at $\omega=9.8$ meV. No other features are apparent for energy transfers up to 18 meV. The peak position is practically independent of Q , but the intensity of the excitation decreases with increasing Q . The solid lines are Gaussian curves plus backgrounds as follows, and well reproduce the experimental spectra for $\omega \geq 3$ meV:

$$I(\omega) = I_0 \exp[-(\omega - \omega_0)^2/\Delta\omega^2] + I_{\text{BG}}(\omega). \quad (1)$$

Here I_0 , ω_0 , $\Delta\omega$, and $I_{\text{BG}}(\omega)$ respectively denote a scaling factor, peak energy, width of the Gaussian, and the background intensity. We assume that $I_{\text{BG}}(\omega) = A\omega + B$, where A and B are constants in each spectrum. The full width at half maximum (FWHM) is evaluated as 2.1–2.6 meV in these spectra. The dotted lines indicate the energy resolution profile plus the background calculated for 9.8 meV. The FWHM of the experimental resolution is 2.0 meV. Therefore, the observed widths in $\text{Cu}_3(\text{P}_2\text{O}_6\text{OD})_2$ are slightly larger than the experimental resolution.

The open circles in Fig. 2(b) represent constant- Q scan spectra measured at $Q=1.3 \text{ \AA}^{-1}$ and several temperatures. Upon heating, the scattering intensities of the excitation are reduced, but the peak position is almost independent of the temperature. Only a slight broadening is apparent at higher temperatures. For example, the FWHMs are respectively 2.5 and 3.1 meV at 5.1 and 286 K. Similar broadening is apparent in $\text{CaCuGe}_2\text{O}_6$, of which the spin system consists of weakly interacting AF dimers.¹⁹ Considering the results described above, we can conclude that the 9.8 meV peak indicates magnetic excitation with small dispersion.

The red open circles in Fig. 3 show constant- ω scan spectra taken at 9.75 meV and 5.1 K. As Q increases, the intensity increases slightly up to 1.3 \AA^{-1} , then decreases rapidly up to 2.5 \AA^{-1} ; it levels off at higher Q . We also show the intensities measured at 4 meV (green closed circles) and

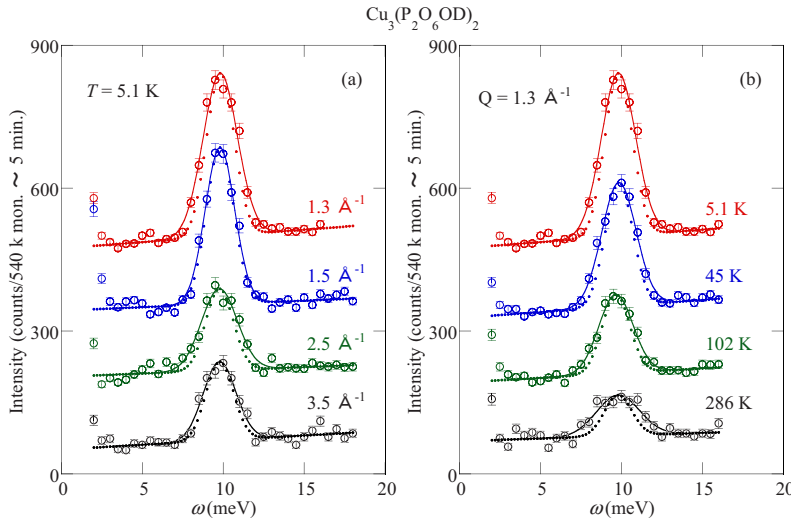


FIG. 2. (Color online) (a) Constant- Q scan spectra indicated by circles at 5.1 K and at (b) $Q=1.3 \text{ \AA}^{-1}$. The solid lines show fitted Gaussian curves plus backgrounds. The dotted lines represent the experimental resolution function. The spectra have been shifted vertically at intervals of 150.

6 meV (blue open circles). The intensities are nearly independent of Q . The average is about 59 and is used as the background intensity for the 9.75 meV data because of the following reason. As shown in Fig. 2, no excitation is seen at 4 and 6 meV. Thus, the intensities at 4 and 6 meV can be regarded as background intensities. In addition, by taking the intensities at $\omega \geq 13$ meV into account, the background intensities seem to depend weakly on ω . Consequently, we used the intensities at 4 and 6 meV as the background intensities for the 9.75 meV excitation. The red circles in Fig. 4 represent the temperature dependence of the energy-integrated intensity of the 9.8 meV peak. The integrated intensity is defined as a scaled value of $I_0 \Delta \omega$. On heating, the integrated intensity decreases slowly at low T and rapidly above 40 K, and levels off at higher T .

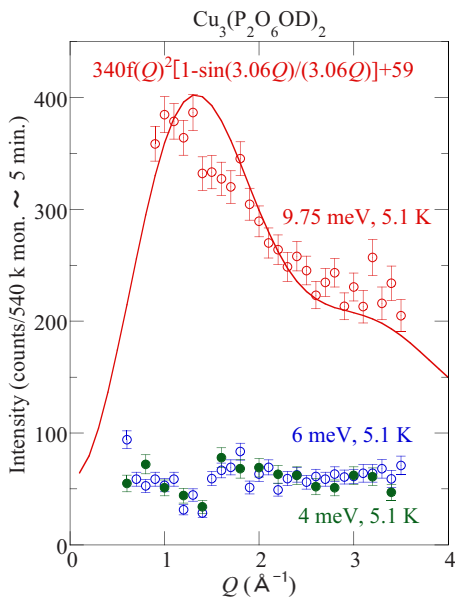


FIG. 3. (Color online) Constant- ω scan spectra at 5.1 K for 9.75 meV (red open circles), 6 meV (blue open circles), and 4 meV (green closed circles). The solid line indicates the calculated Q dependence of the isolated AF dimer model.

We compare the experimental results in Figs. 3 and 4 with the isolated AF dimer model. The Q dependence of the scattering intensity for unpolarized neutrons is expressed as²²

$$I_D(Q) = I_{D0} f(Q)^2 [1 - \sin(d_D Q)/(d_D Q)] + I_{BG}. \quad (2)$$

In that equation, I_{D0} , $f(Q)$, d_D , and I_{BG} respectively represent a scaling factor, an atomic magnetic form factor,²³ an intradimer spin separation, and the background intensity. The solid line in Fig. 3 represents a fit with Eq. (2) using $d_D = 3.06 \text{ \AA}$, and reproduces roughly overall features of the experimental result. The value 3.06 \AA is the distance between two spins on Cu2 sites coupled by the J_1 interaction. Therefore, the result in Fig. 3 is consistent with the idea that the two Cu2 spins coupled by the J_1 interaction form the AF dimer. The T dependence of the integrated intensity in Fig. 4 is proportional to $I_D(T)$, which is given as

$$I_D(T) = 1/[1 + 3 \exp(-\Delta/T)], \quad (3)$$

where Δ is an energy gap between a singlet ground state and triplet excited states. The value of Δ can be regarded as 114 K (9.8 meV) in $\text{Cu}_3(\text{P}_2\text{O}_6\text{OD})_2$. The solid line in Fig. 4

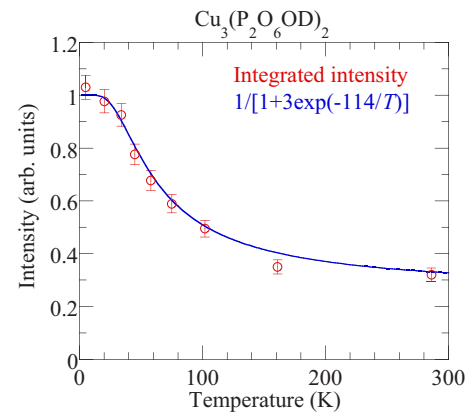


FIG. 4. (Color online) Temperature dependence of the integrated intensity of the 9.8 meV peak (circles). The solid line shows the calculated T dependence of the isolated AF dimer model.

indicates the calculated curve and is consistent with the experimental result.

The gap value obtained using the present INS measurements (9.8 meV) is slightly larger than that obtained using the previous calculation of magnetization (8.1 meV). Note that we did not obtain the gap value of 8.1 meV from the experimental results. Therefore, discrepancy between the gap values resulted from inaccurate values of J_1 and J_2 . For that reason, we have reevaluated J_1 and J_2 to reproduce not only the temperature dependence of the susceptibility and magnetic-field dependence of the magnetization but also the gap value determined by the INS measurements in the following procedure. We calculated magnetizations for several values of $j \equiv J_2/J_1$ at the low temperature of $t \equiv T/J_1 = 0.02$. In each calculated magnetization, a value of J_1 was determined in order to reproduce the gap value. Among the calculated magnetizations, we chose the calculated magnetization that was able to reproduce the experimental one best. We obtained $J_1 = 111$ K and $j = 0.27$ ($J_2 = 30$ K). Then, we compared the calculated susceptibility of these values [the green curve with \triangle in Fig. 5(a)] with the experimental one [the red curve with \circ in Fig. 5(a)]. The two curves are not mutually contradictory, although a small discrepancy is apparent at high T . Finally, we calculated magnetization with $J_1 = 111$ K and $j = 0.27$ at $t = 1.6/111 = 0.0144$ [the green curve with \triangle in Fig. 5(b)], which was consistent with the experimental one [the red curve with \circ in Fig. 5(b)] except for a slight discrepancy around 10 T.

As a result, as was expected, we observed the gap that generated the 1/3 magnetization plateau. Because of the consistency between the experimental results and expected results in the AF dimer model, the main origin of the 9.8 meV magnetic excitation is the singlet-triplet gap of the AF dimer formed by the J_1 interaction. The J_2 interaction, however, undoubtedly exists.¹⁷ Other interactions such as the J_2 interaction cause a small dispersion of the dimer excitation and slightly broaden the peak width. We briefly comment on magnetic excitation of spins on the Cu1 sites. As described, the Cu1 spins are regarded to form the AF uniform chain with the interaction of $J_{\text{eff}} \sim J_2^2/J_1$. Consequently, most of the magnetic excitations of the Cu1 spins must appear around $\omega = 0$. In addition, because the value of J_{eff} is small (8.0 K = 0.69 meV), we were unable to detect the magnetic excitations of the Cu1 spins in the setup of the present experiment.

IV. CONCLUSION

We performed inelastic neutron scattering measurements on a powder sample of $\text{Cu}_3(\text{P}_2\text{O}_6\text{OD})_2$ whose spin system is the spin-1/2 trimer chain with J_1 - J_2 - J_2 interactions, where J_1 and J_2 indicate two kinds of AF exchange interaction parameters. A well-defined symmetric inelastic peak was observed at $\omega = 9.8$ meV in constant- Q scan spectra. The peak position is nearly independent of Q and temperature. The peak is slightly wider than the experimental resolution. The Q dependence of the peak intensity and the temperature dependence of the integrated intensity are consistent with the calculated values in the AF dimer model. We confirmed that the energy gap, which generates the 1/3 magnetization plateau,

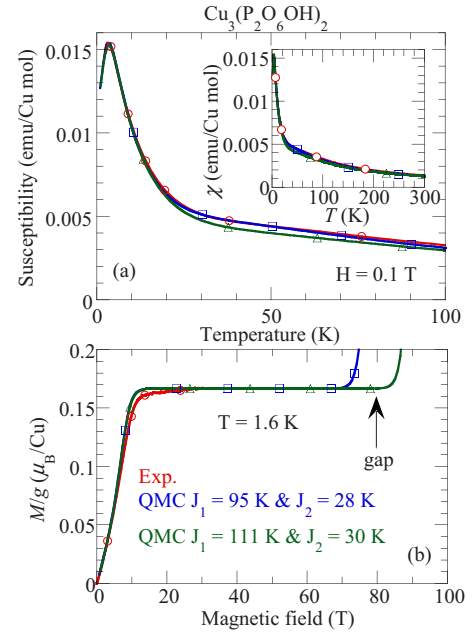


FIG. 5. (Color online) (a) The temperature dependence of magnetic susceptibility χ in 0.1 T and magnetic-field dependence of magnetization M at 1.6 K. Red, blue, and green curves with \circ , \square , and \triangle , respectively, are experimental results of $\text{Cu}_3(\text{P}_2\text{O}_6\text{OH})_2$, the previous QMC results for the spin-1/2 trimer chains with $J_1 = 95$ and $J_2 = 28$ K, and the new QMC results with $J_1 = 111$ and $J_2 = 30$ K. The inset in (a) shows the same results up to 300 K. The red and blue curves overlap with each other in (a); the blue and green curves below 70 T overlap with each other in (b). It is difficult to distinguish the overlapped curves. Therefore, in order to indicate existence of plural curves, we draw the symbols (\circ , \square , and \triangle) representing some points of the experimental and QMC results. The arrow in (b) indicates the gap value. The g factor was determined as 2.12 from ESR measurement at room temperature.

exists at 9.8 meV (114 K), and that the main origin of the gap is the singlet-triplet excitation of the AF dimer formed by the dominant J_1 interaction. Other interactions such as the J_2 interaction, however, cannot be ignored completely. The interactions cause a small dispersion of the dimer excitation and slightly broaden the peak width. We obtained the AF exchange interaction parameters $J_1 = 111$ K and $J_2 = 30$ K which reproduced the gap value as well as the magnetization.

ACKNOWLEDGMENTS

We are grateful to S. Matsumoto for synthesis of samples and x-ray diffraction measurements, and to M. Kaise for x-ray diffraction measurements. The neutron scattering experiments were carried out in the framework of JAEA Users' Program and within the NIMS-RIKEN-JAEA Collaborative Research Program on Quantum Beam Science and Technology. This work was supported by grants from NIMS and by a Grant-in-Aid for Scientific Research (c) (No. 18540359) from the Ministry of Education, Culture, Sports, Science, and Technology of Japan.

*hase.masashi@nims.go.jp

- ¹K. Hida, J. Phys. Soc. Jpn. **63**, 2359 (1994).
- ²M. Oshikawa, M. Yamanaka, and I. Affleck, Phys. Rev. Lett. **78**, 1984 (1997).
- ³Y. Narumi, M. Hagiwara, R. Sato, K. Kindo, H. Nakano, and M. Takahashi, Physica B **246**, 509 (1998); Y. Narumi, K. Kindo, M. Hagiwara, H. Nakano, A. Kawaguchi, K. Okunishi, and M. Kohno, Phys. Rev. B **69**, 174405 (2004).
- ⁴W. Shiramura, K. Takatsu, B. Kurniawan, H. Tanaka, H. Uekusa, Y. Ohashi, K. Takizawa, H. Mitamura, and T. Goto, J. Phys. Soc. Jpn. **67**, 1548 (1998).
- ⁵K. Katsumata, H. Hori, T. Takeuchi, M. Date, A. Yamagishi, and J. P. Renard, Phys. Rev. Lett. **63**, 86 (1989).
- ⁶Y. Ajiro, T. Goto, H. Kikuchi, T. Sakakibara, and T. Inami, Phys. Rev. Lett. **63**, 1424 (1989).
- ⁷M. Hase, I. Terasaki, K. Uchinokura, M. Tokunaga, N. Miura, and H. Obara, Phys. Rev. B **48**, 9616 (1993).
- ⁸H. Kageyama, K. Yoshimura, R. Stern, N. V. Mushnikov, K. Onizuka, M. Kato, K. Kosuge, C. P. Slichter, T. Goto, and Y. Ueda, Phys. Rev. Lett. **82**, 3168 (1999).
- ⁹J. P. Renard, M. Verdaguer, L. P. Regnault, W. A. C. Erkelens, J. Rossatmignod, and W. G. Stirling, Europhys. Lett. **3**, 945 (1987).
- ¹⁰M. Hase, I. Terasaki, and K. Uchinokura, Phys. Rev. Lett. **70**, 3651 (1993); M. Hase, I. Terasaki, Y. Sasago, K. Uchinokura, and H. Obara, *ibid.* **71**, 4059 (1993); M. Hase, N. Koide, K. Manabe, Y. Sasago, K. Uchinokura, and A. Sawa, Physica B **215**, 164 (1995); M. Hase, K. Uchinokura, R. J. Birgeneau, K. Hirota, and G. Shirane, J. Phys. Soc. Jpn. **65**, 1392 (1996).
- ¹¹K. Takatsu, W. Shiramura, and H. Tanaka, J. Phys. Soc. Jpn. **66**, 1611 (1997).
- ¹²H. Kikuchi, Y. Fujii, M. Chiba, S. Mitsudo, T. Idehara, T. Tonegawa, K. Okamoto, T. Sakai, T. Kuwai, and H. Ohta, Phys. Rev. Lett. **94**, 227201 (2005).
- ¹³M. Hase, M. Kohno, H. Kitazawa, O. Suzuki, K. Ozawa, G. Kido, M. Imai, and X. Hu, Phys. Rev. B **72**, 172412 (2005).
- ¹⁴Ch. Rüegg, M. Oettli, J. Schefer, O. Zaharko, A. Furrer, H. Tanaka, K. W. Kramer, H. U. Gudel, P. Vorderwisch, K. Habicht, T. Polinski, and M. Meissner, Phys. Rev. Lett. **93**, 037207 (2004).
- ¹⁵B. Kurniawan, H. Tanaka, K. Takatsu, W. Shiramura, T. Fukuda, H. Nojiri, and M. Motokawa, Phys. Rev. Lett. **82**, 1281 (1999).
- ¹⁶H. Ohta, S. Okubo, T. Kamikawa, T. Kunimoto, Y. Inagaki, H. Kikuchi, T. Saito, M. Azuma, and M. Takano, J. Phys. Soc. Jpn. **72**, 2464 (2003).
- ¹⁷M. Hase, M. Kohno, H. Kitazawa, N. Tsujii, O. Suzuki, K. Ozawa, G. Kido, M. Imai, and X. Hu, Phys. Rev. B **73**, 104419 (2006).
- ¹⁸R. Baies, V. Caignaert, V. Pralong, and B. Raveau, Inorg. Chem. **44**, 2376 (2005).
- ¹⁹A. Zheludev, G. Shirane, Y. Sasago, M. Hase, and K. Uchinokura, Phys. Rev. B **53**, 11642 (1996).
- ²⁰See references in H. G. Evertz, Adv. Phys. **52**, 1 (2003).
- ²¹O. F. Syljuåsen and A. W. Sandvik, Phys. Rev. E **66**, 046701 (2002).
- ²²A. Furrer and H. U. Gudel, Phys. Rev. Lett. **39**, 657 (1977).
- ²³P. J. Brown, in *International Tables for Crystallography*, edited by A. J. C. Wilson (Kluwer Academic, Dordrecht, 1995), Vol. C, p. 391.